Dyes and Pigments 82 (2009) 286–292

Contents lists available at ScienceDirect

Dyes and Pigments

journal homepage: www.elsevier.com/locate/dyepig

The photoinduced surface-relief-grating formation behavior of side-chain azo polymers with narrow M_r distribution

Dongrui Wang, Yaning He, Wei Deng, Xiaogong Wang*

Department of Chemical Engineering, Laboratory for Advanced Materials, Tsinghua University, Beijing 100084, PR China

ARTICLE INFO

Article history:
Received 11 November 2008
Received in revised form
14 January 2009
Accepted 18 January 2009
Available online 29 January 2009

Keywords:
Azo polymer
Atom transfer radical polymerization
Azo-coupling reaction
Surface-relief-gratings
Molecular weight
Narrow-dispersed

ABSTRACT

Surface-relief-grating formation induced by Ar^+ laser irradiation was studied using two series of side-chain azo polymers with narrow M_r distribution. The methacrylate-based azo polymers were synthesized using an approach that combined atom transfer radical polymerization and post-polymerization azo-coupling. The azo polymers were characterized using spectroscopic methods, GPC measurement as well as thermal analysis. The surface-relief-grating formation behavior of the azo polymers was examined by irradiating thin polymer films with interfering Ar^+ laser beams. Whilst the M_r of the two polymers had no effect upon surface-relief-grating inscription rate, in contrast, different rates of grating formation and modulation depths were observed for the two polymers.

1. Introduction

Since it was first reported in 1995, the surface-relief-grating (SRG) formation of azo polymer films has attracted considerable attention [1–4]. By exposing azo polymer films to interfering laser beams, SRGs can be inscribed on the film surfaces at a temperature substantially below the glass transition temperature (T_g) of the material. The surface patterns obtained through this all-optical process can be erased by thermal or optical methods and the writing–erasing process is completely reversible. In most cases, the writing and erasing cycle can be repeated for many times without causing damage to surfaces. Different models and theories have been proposed to explain the SRG formation mechanism, which consider the internal pressure gradient caused by an isomerization-driven free volume expansion in the bulk [5], the force based on the dipolar interaction of the azo chromophores with the optically induced electric field gradient [6,7], the translational wormlike diffusion caused by the photoisomerization of the azobenzene chromophores [8], and the mean-field force related to the molecule alignment [9]. Recently, the photomechanical effect occurring in thin films of azo polymers has been proposed as a new candidate mechanism to explain the SRG formation [10–12]. Although it is generally agreed that the repeated *trans–cis–trans* isomerization upon the light irradiation plays a key role in the process, the exact mechanism of SRG formation is still an unsettled problem. This photo-processing method can be potentially applied in areas such as holographic storage [3,4], liquid crystal anchoring [13], waveguide couplers [14], and fabrication of complicated surface structures [15].

In order to fully understand the general features of this unusual photoinduced effect, the factors affecting the SRG formation have been extensively investigated since this phenomenon was discovered. It has been reported that the photoinduced dynamic process depends on the intensity and polarization state of the interfering beams, polymer structures, molecular weight, and thickness of the films [3,4]. The influences of the polymer architectures, such as chromophore structures, degree of functionalization, and backbone type, have been studied by using azo polyacrylates, azo polyesters, and epoxy-based azo polymers [3,16–18]. The M_r effect on SRG formation has been investigated through different approaches; an azo polymer (PDR1A) was blended with poly(methyl methacrylate) (PMMA) of varying M_rs [5]. The SRG inscription study shows that the surface deformation can be achieved only when the M_r of PMMA is low. The inhibition of SRG formation has been attributed to the PMMA chain entanglements. A series of azobenzene-containing copolymers P(MMA-*co*-DR13M) with different M_rs have been prepared. It is observed that the polymers with lower M_r form SRGs having higher diffraction efficiency, which is an indication of

* Corresponding author. Tel.: +86 10 62784561; fax: +86 10 62770304.
E-mail address: wxg-dce@mail.tsinghua.edu.cn (X. Wang).

0143-7208/$ – see front matter © 2009 Elsevier Ltd. All rights reserved.
doi:10.1016/j.dyepig.2009.01.012

the deeper surface modulation [19]. Recently, low-M_r molecular glasses containing azobenzene moieties have been prepared and their SRG formation ability has been studied [20–22]. Compared to azo polymers, the molecular glasses can form SRG more efficiently owning to the higher chromophore density and easier mass–motion ability. Besides M_r the molecular mass distribution is also an important factor in terms of polymer properties. In previous studies, the azo polymers used for SRG investigation were synthesized by conventional radical polymerization or polycondensation, which possessed broad M_r distribution. To our knowledge, study of the SRG formation behavior by using narrow-dispersed azo polymers has rarely been reported in the literature.

In this work, two series of methacrylate-based azo polymers (PNTAZO, PCNAZO) with different M_rs were prepared. The polymers having narrow M_r distributions were synthesized through atom transfer radical polymerization (ATRP) and post-polymerization azo-coupling reaction. ATRP is well known for its ability to control both molecular mass and distribution [23]. In the current study, it was used to obtain a series of narrow-dispersed aniline-containing precursor polymers with different M_rs. Then, the two series of azo polymers were synthesized through azo-coupling reactions between the precursor polymers and corresponding diazonium salts. The synthesis, characterization and SRG formation behavior of these two series of azo polymers will be discussed in the following sections in detail.

2. Experimental

2.1. Materials and measurements

1,1,4,7,10,10-Hexamethyltriethylenetetramine (HMTETA) (97%, Aldrich), *N*-ethyl-*N*-hydroxyethylaniline (96%, Acros), and 4-aminobenzonitrile (98%, Acros) were used without further purification. CuCl (99%, Aldrich) was washed orderly with excess acetic acid, ethanol and ether, and then dried. Acetone was freshly distilled before use. All other reagents and solvents were commercial products and used as received. M_rs and M_r distributions were determined using gel permeation chromatography (GPC) at 25 °C using THF as the eluent (1 mL/min). The instrument was equipped with a refractive index (RI) detector (Wyatt Optilab rEX) and fitted with a PLgel 5 μm mixed-D column calibrated using linear polystyrene standards. The M_rs of PEMA were obtained from the response of a laser light scattering detector (Wyatt miniDAWN) that was connected to the GPC line with a laser source of 633 nm. The d*n*/d*c* value of PEMA was measured using the Wyatt Optilab rEX. For polymers whose M_r could not be obtained by the above method, polystyrene standards with dispersity of 1.08–1.12 obtained from Waters were employed to calibrate the instrument. ^{1}H NMR spectra were recorded using a JEOL JNM-ECA300 NMR spectrometer. Thermal phase transitions of the polymers were tested using TA Instruments DSC 2920 with a heating rate of 10 °C/min in nitrogen atmosphere. UV–vis absorption spectra were recorded on a Perkin–Elmer Lamba Bio-40 spectrometer. The surface images of the surface-relief-gratings were monitored using Atomic Force Microscopy (AFM, Nanoscope IIIa, tapping mode).

2.2. PEMA obtained through ATRP

The monomer 2-(*N*-ethyl-*N*-phenylamino)ethyl methacrylate (EMA) was synthesized by esterification according to the procedure published previously [24]. Four PEMA samples with different M_rs (**a1**, **a2**, **a3**, **a4**) were prepared through ATRP. The synthesis of **a2** is given here as a typical example: *p*-toluenesulfonyl chloride (19.06 mg, 0.1 mmol) and CuCl (9.9 mg, 0.1 mmol) were added to a Schlenk flask. It was then degassed and back-filled with argon three times. Following this step, deoxygenated acetone (2 mL), EPAEMA (1.165 g, 5 mmol) and HMTETA (27.2 μL, 0.1 mmol) were added in turn via gas-tight syringes which had been previously purged with argon. After degassing by three freeze–pump–thaw cycles, the flask was immersed in an oil bath preheated to 50 °C for 20 h. Before the reaction was stopped by diluting with THF, a sample was removed for ^{1}H NMR analysis to determine the conversion of the monomer. Then the mixture was passed through an alumina column to remove catalyst. The filtrate was concentrated and poured into an excess amount of petrol ether. The precipitate was collected by filtration, washed with petrol ether and then dried in a vacuum oven at 45 °C for 24 h. Conversion = 87%. d*n*/d*c* = 0.154 mL/g. M_n (GPC–LS) = 19 900, M_w/M_n (GPC–LS) = 1.06. ^{1}H NMR (DMF-d_7) δ (ppm): 0.70–1.05 (m, CH_3, 3H), 1.08 (br, CH_3, 3H), 1.55–1.95 (m, CH_2, 2H), 3.41 (br, CH_2, 2H), 3.57 (br, CH_2, 2H), 4.07 (br, CH_2, 2H), 6.60 (br, Ar-H, 1H), 6.78 (br, Ar-H, 2H), 7.16 (br, Ar-H, 2H). The other three PEMA samples were prepared under the same procedure. The analytical results of these PEMA specimens are listed below.

a1, Conversion = 56%. d*n*/d*c* = 0.154 mL/g. M_n (GPC–LS) = 11 200, M_w/M_n (GPC–LS) = 1.08. ^{1}H NMR (DMF-d_7) δ (ppm): 0.70–1.05 (m, CH_3, 3H), 1.10 (br, CH_3, 3H), 1.55–1.95 (m, CH_2, 2H), 3.42 (br, CH_2, 2H), 3.58 (br, CH_2, 2H), 4.07 (br, CH_2, 2H), 6.61 (br, Ar-H, 1H), 6.78 (br, Ar-H, 2H), 7.17 (br, Ar-H, 2H).

a3, Conversion = 76%. d*n*/d*c* = 0.154 mL/g. M_n (GPC–LS) = 30 000, M_w/M_n (GPC–LS) = 1.08. ^{1}H NMR (DMF-d_7) δ (ppm): 0.70–1.05 (m, CH_3, 3H), 1.08 (br, CH_3, 3H), 1.55–1.95 (m, CH_2, 2H), 3.40 (br, CH_2, 2H), 3.56 (br, CH_2, 2H), 4.06 (br, CH_2, 2H), 6.61 (br, Ar-H, 1H), 6.79 (br, Ar-H, 2H), 7.17 (br, Ar-H, 2H).

a4, Conversion = 93%. d*n*/d*c* = 0.154 mL/g. M_n (GPC–LS) = 46 600, M_w/M_n (GPC–LS) = 1.10. ^{1}H NMR (DMF-d_7) δ (ppm): 0.70–1.05 (m, CH_3, 3H), 1.08 (br, CH_3, 3H), 1.55–1.95 (m, CH_2, 2H), 3.40 (br, CH_2, 2H), 3.56 (br, CH_2, 2H), 4.06 (br, CH_2, 2H), 6.59 (br, Ar-H, 1H), 6.77 (br, Ar-H, 2H), 7.16 (br, Ar-H, 2H).

2.3. Synthesis of PNTAZO

PNTAZO (**b1**, **b2**, **b3**, **b4**) were prepared by azo-coupling reaction between PEMA and diazonium salt of 4-nitroaniline. The synthesis of **b1** is given below as a typical example. A diazonium salt solution of 4-nitroaniline was prepared by adding an aqueous solution of sodium nitrite (0.1 g, 1.45 mmol) dropwise into a solution of 4-nitroaniline (0.173 g, 1.25 mmol) in a homogeneous mixture of sulfuric acid (0.25 mL) and glacial acetic acid (5 mL). The mixture was stirred at 0 °C for 5 min. Then the diazonium salt solution was added dropwise into a solution of **a1** (0.233 g, 1 mmol in terms of the aniline group) in DMF (20 mL) at 0 °C. After the reaction was carried out at 0 °C for 12 h, the solution was poured into an excess amount of water. The precipitate was collected by filtration and washed with a large amount of water. After drying, the product was dissolved in THF and then the solution was added dropwise into an excess amount of petrol ether with stirring. The precipitate was collected by filtration and dried in a vacuum oven at 40 °C for 24 h. Yield: 0.351 g, 92%. M_n (GPC) = 8500, M_w/M_n (GPC) = 1.13. ^{1}H NMR (DMF-d_7) δ (ppm): 0.65–1.05 (m, CH_3, 3H), 1.08 (br, CH_3, 3H), 1.60–2.00 (m, CH_2, 2H), 3.46 (br, CH_2, 2H), 3.71 (br, CH_2, 2H), 4.13 (br, CH_2, 2H), 6.86 (br, Ar-H, 2H), 7.79 (br, Ar-H, 4H), 8.23 (br, Ar-H, 2H). The other three PNTAZO specimens **b2**, **b3**, **b4** were prepared under the same conditions using **a2**, **a3**, **a4** as precursor polymers, respectively. The analytical results of these PNTAZO samples are listed below.

b2, Yield: 0.340 g, 89%. M_n (GPC) = 14 800, M_w/M_n (GPC) = 1.20. ^{1}H NMR (DMF-d_7) δ (ppm): 0.60–1.00 (m, CH_3, 3H), 1.06 (br, CH_3, 3H), 1.60–2.00 (m, CH_2, 2H), 3.44 (br, CH_2, 2H), 3.69 (br, CH_2, 2H), 4.11 (br, CH_2, 2H), 6.85 (br, Ar-H, 2H), 7.78 (br, Ar-H, 4H), 8.22 (br, Ar-H, 2H).

b3, Yield: 0.336 g, 88%. M_n (GPC) = 20 000, M_w/M_n (GPC) = 1.16. ^{1}H NMR (DMF-d_7) δ (ppm): 0.65–1.05 (m, CH_3, 3H), 1.07 (br, CH_3, 3H), 1.60–2.05 (m, CH_2, 2H), 3.45 (br, CH_2, 2H), 3.70 (br, CH_2, 2H), 4.12 (br, CH_2, 2H), 6.85 (br, Ar-H, 2H), 7.79 (br, Ar-H, 4H), 8.22 (br, Ar-H, 2H).

b4, Yield: 0.280 g, 73%. M_n (GPC) = 26 000, M_w/M_n (GPC) = 1.25. ^{1}H NMR (DMF-d_7) δ (ppm): 0.65–1.05 (m, CH_3, 3H), 1.08 (br, CH_3, 3H), 1.60–2.05 (m, CH_2, 2H), 3.45 (br, CH_2, 2H), 3.71 (br, CH_2, 2H), 4.13 (br, CH_2, 2H), 6.85 (br, Ar-H, 2H), 7.79 (br, Ar-H, 4H), 8.23 (br, Ar-H, 2H).

2.4. Synthesis of PCNAZO

PCNAZO (**c1**, **c2**, **c3**, **c4**) were synthesized through the azo-coupling reactions between **a1**, **a2**, **a3**, **a4** and the diazonium salt of 4-aminobenzotrile. The procedure and conditions were the same as the preparation of PNTAZO except that 4-aminobenzotrile was used instead of 4-nitroaniline. The analytical results of these PCNAZO samples are listed below.

c1, Yield: 0.334 g, 92%. M_n (GPC) = 12 300, M_w/M_n (GPC) = 1.17. ^{1}H NMR (DMF-d_7) δ (ppm): 0.45–1.00 (m, CH_3, 3H), 1.08 (br, CH_3, 3H), 1.50–2.00 (m, CH_2, 2H), 3.40–3.90 (m, CH_2, 4H), 4.10 (br, CH_2, 2H), 6.86 (br, Ar-H, 2H), 7.83 (br, Ar-H, 6H).

c2, Yield: 0.342 g, 94%. M_n (GPC) = 18 000, M_w/M_n (GPC) = 1.19. ^{1}H NMR (DMF-d_7) δ (ppm): 0.45–1.00 (m, CH_3, 3H), 1.07 (br, CH_3, 3H), 1.50–2.00 (m, CH_2, 2H), 3.40–3.90 (m, CH_2, 4H), 4.12 (br, CH_2, 2H), 6.87 (br, Ar-H, 2H), 7.84 (br, Ar-H, 6H).

c3, Yield: 0.337 g, 93%. M_n (GPC) = 24 500, M_w/M_n (GPC) = 1.29. ^{1}H NMR (DMF-d_7) δ (ppm): 0.45–1.00 (m, CH_3, 3H), 1.07 (br, CH_3, 3H), 1.50–2.00 (m, CH_2, 2H), 3.40–3.90 (m, CH_2, 4H), 4.11 (br, CH_2, 2H), 6.86 (br, Ar-H, 2H), 7.82 (br, Ar-H, 6H).

c4, Yield: 0.341 g, 94%. M_n (GPC) = 33 800, M_w/M_n (GPC) = 1.35. ^{1}H NMR (DMF-d_7) δ (ppm): 0.45–1.00 (m, CH_3, 3H), 1.07 (br, CH_3, 3H), 1.50–2.00 (m, CH_2, 2H), 3.40–3.90 (m, CH_2, 4H), 4.12 (br, CH_2, 2H), 6.87 (br, Ar-H, 2H), 7.84 (br, Ar-H, 6H).

2.5. Inscription of surface-relief-gratings

The azo polymers were dissolved in DMF to obtain solutions with concentrations about 10 wt%. Then the solutions were filtered with 0.45 μm syringe membranes and spin-coated onto clean glass slides with the rate of 1000 rpm. The thicknesses of the films were all controlled to be about 1.0 μm. After drying at 70 °C under vacuum for 48 h, the films were stored in a desiccator for further studies. The experimental setup for SRG fabrication was similar to those reported before [1,2,17]. A linearly polarized Ar^+ laser beam (488 nm, 150 mW/cm^2) was used as the light source. The Ar^+ laser beam was split by a mirror and the reflected half beam coincided with the other half on the film surface. SRGs were optically inscribed on the polymer films with p-polarized interfering laser beams. The progression of the grating inscription was monitored by measuring the intensity variation of the first-order diffraction beam of a low-power unpolarized He–Ne laser beam (633 nm) in transmission mode. The surface profiles of the resulting gratings were recorded by using AFM in the tapping mode.

3. Results and discussion

The synthetic route to prepare series of PNTAZO and PCNAZO is shown in Fig. 1. PNTAZO has the same repeat unit structure as PDR1M,which has been prepared by typical radical polymerization [25]. Due to the inhibition of the azo groups to the free radicals, azo polymers with high M_r could hardly be prepared through radical polymerization of monomers containing aminoazobenzene moieties [25,26]. Our failed attempts to obtain PNTAZO via ATRP of

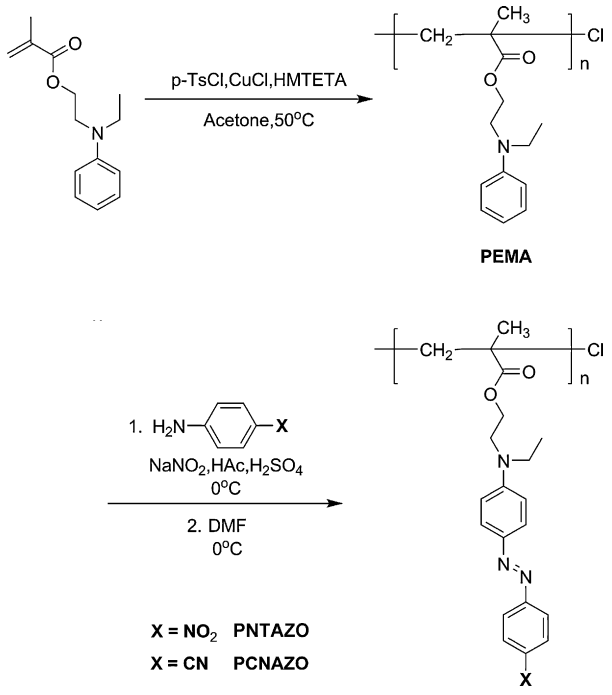

Fig. 1. Synthetic route for preparing azo polymers.

2-(*N*-ethyl-*N*-(4-(4-nitrophenylazo)phenyl)amino)ethyl methacrylate also confirm this point. Therefore, the two-stage route was used for the azo polymer preparation, in which precursor polymers (PEMA) were prepared by ATRP, and then the azo polymers were synthesized by post-polymerization azo-coupling reaction. The post-polymerization azo-coupling reaction can have a high reaction yield to reach about 100% [27,28]. This reaction route also has the advantage to avoid possible side reactions between the free radicals and the azo chromophores.

The precursor polymers (PEMA) were obtained through ATRP by using similar conditions reported for the polymerization of poly(2-(diethylamino)ethyl methacrylate) [29]. Four PEMA samples with different M_rs were synthesized by adjusting the feed ratio of the monomer to the initiator. The preparation conditions and M_r parameters are given in Tables 1 and 2. M_r was determined by GPC using the standard GPC–LS combination method. The GPC traces are shown in Fig. 2, which show that the polymers have a narrow M_r distribution. The theoretical M_ns, which are calculated from the feed ratios by assuming the living polymerization condition, are also listed in Table 1. The calculated values are obviously lower than the M_r obtained from GPC–LS, which could be attributed to the low initiator efficiency. It could be caused by the formation of sulfonyl

Table 1
Experimental conditions[a] and conversion of PEMA synthesized by the ATRP method.

Sample	$[M]_0/[I]_0$[b]	Time (h)	Conv.[c] (%)	M_n[d] (cal)
a1	50	10	56	6700
a2	50	20	87	10 300
a3	100	20	76	17 900
a4	150	20	93	32 700

[a] $[Initiator]_0:[Cu(I)Cl]_0:[HMTETA]_0 = 1:1:1$. *p*-Toluenesulfonyl chloride used as initiator and acetone used as solvent. Polymerization temperature is 50 °C.
[b] Feed molar ratio of the monomer $[M]_0$ to the initiator $[I]_0$.
[c] Determined by ^{1}H NMR.
[d] Number average molecular weights calculated according to $M_n = 190.6 + 233 \times conv. \times [M]_0/[I]_0$, where 190.6 and 233 are the molecular weights of initiator and monomer, respectively.

Table 2
The molecular weight data and glass transition temperatures of PEMA.

Sample	M_n (GPC–LS)[a]	M_w/M_n (GPC–LS)[a]	M_n (GPC)[b]	M_w/M_n (GPC)[b]	T_g[c] (°C)
a1	11 200	1.08	5900	1.11	35
a2	19 900	1.06	9900	1.09	36
a3	30 000	1.08	14 300	1.10	37
a4	46 600	1.10	21 300	1.11	38

[a] Determined by GPC, using an LS–RI combination method to calculate actual molecular weights.
[b] Determined by GPC, the column was calibrated with PS standards.
[c] Determined by DSC.

esters from sulfonyl chlorides during the early stage of the polymerization [30].

The GPC traces of PNTAZO and PCNAZO derived from PEMA are also given in Fig. 2. After the azo-coupling reactions, the peaks shift to higher molar mass regions along with disappearance of the peaks of the PEMA precursor. All of the obtained azo polymers exhibit narrow distributions of M_r. On the other hand, a small shoulder is visible in high M_r side, which could arise from the possible aggregation of polymer chains in THF. Owing to the strong dipole–dipole interaction between the azo chromophores, aggregation of polymeric chains through the van der Waals' interaction could occur in THF eluent to some degree.

As the dn/dc values of the solutions could not be properly measured due to the high polarizability of the azo polymers, it was unable to obtain the M_r of PNTAZO and PCNAZO by GPC–LS method. The M_r and mass distributions of the polymers were estimated by the two alternative methods. In the first case, they were estimated from the M_r of PEMA by using the degree of functionalization (DF) obtained from the ^{1}H NMR. The M_rs of PNTAZO and PCNAZO obtained by this method are given in Table 3. As the DFs are all about 100%, the M_r distributions should be similar to the corresponding PEMA samples. In the second case, the M_rs and M_r distributions were obtained from GPC by using monodispersed polystyrene (PS) as standard to calibrate the instrument. The M_rs and M_r distributions of PNTAZO and PCNANO obtained by this

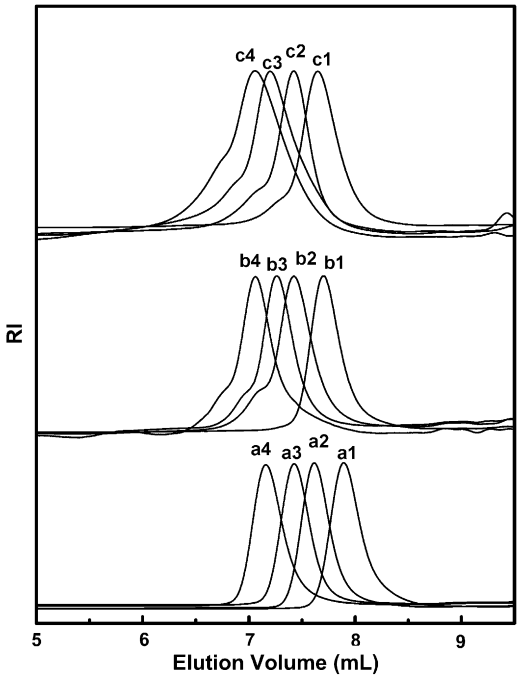

Fig. 2. GPC traces of the precursor polymers and azo polymers.

Table 3
Characterization data of azo polymers.

Sample	Composition	M_n[a] (cal)	M_n (GPC)[b]	M_w/M_n (GPC)[b]	T_g[c] (°C)
b1	PNTAZO	18 400	8500	1.13	119
b2	PNTAZO	32 600	14 800	1.20	123
b3	PNTAZO	49 200	20 000	1.16	126
b4	PNTAZO	76 400	26 000	1.25	129
c1	PCNAZO	17 400	12 300	1.17	110
c2	PCNAZO	30 900	18 000	1.19	117
c3	PCNAZO	46 600	24 500	1.29	118
c4	PCNAZO	72 400	33 800	1.35	120

[a] Calculated based on the M_n (GPC–LS) data of the precursor polymers using the azo-coupling reaction conversions of 100% estimated from ^{1}H NMR.
[b] Determined by GPC analyses calibrated with PS standards.
[c] Determined by DSC.

method are also summarized in Table 3. Because the molecular structures of the azo polymers are significantly different with PS, the M_rs obtained by this method should have deviations from the actual values. Therefore, in the following sections, the M_rs estimated from PEMA will be used for the discussions.

The polymer structures were confirmed by the spectroscopic analyses. Fig. 3 shows the ^{1}H NMR spectra of monomer EMA, PEMA (**a1**), PNTAZO (**b1**) and PCNAZO (**c1**). The spectra of other PEMA, PNTAZO and PCNAZO with different M_rs are very similar. In Fig. 3A, there are two resonance signals of vinyl protons at 5.5 and 6.1 ppm and one resonance signal of methyl protons adjacent to the vinyl group at 1.9 ppm. After polymerization, the three resonance signals disappear completely while new resonance signals at 1.6–2.0 and 0.7–1.0 ppm appear (Fig. 3B), which indicates the accomplished polymerization. The high conversion of the post-polymerization azo-coupling reaction can be seen by comparing Fig. 3B to C and D. The 6.6 ppm resonance, corresponding to the protons at the *para* positions of the anilino moieties of PEMA, disappears completely after the azo-coupling reactions. Meanwhile, the resonances from the *ortho* and *meta* protons of the anilino moieties shift to the lower magnetic field (6.9 ppm and 7.8 ppm in Fig. 3C and D). It is caused by the presence of the electron-withdrawing groups introduced after the azo-coupling reaction. These spectral variations indicate that the post-polymerization azo-coupling reactions exclusively occur at the *para* positions of aniline moieties and the conversion of the reaction is nearly 100%.

The phase transitions of PNTAZO and PCNAZO with different M_rs were studied by the differential scanning calorimetry (DSC). The DSC curves from the second heating rounds are given in Fig. 4. All the polymers show the relaxation behavior of a typical amorphous substance. The glass transition temperatures (T_gs) obtained by DSC are listed in Table 3. As it can be seen, higher M_rs lead to higher values of T_g for the same series of the polymers although the differences are not significant (within 10 °C). For PNTAZO, the T_g increases from 119 to 129 °C as the M_r increases from 18 400 to 76 400 g/mol. The result is comparable with the T_g of 105.6 °C for PDR1M ($M_n = 9700$) given in a previous report [26]. For PCNAZO, the T_g increases from 110 to 120 °C as the M_r increases from 17 400 to 72 400 g/mol. For the azo polymers obtained from the same-batch PEMA, the T_g of PNTAZO is slightly higher than that of PCNAZO.

The UV–vis absorption spectra of PNTAZO and PCNAZO in DMF solutions are shown in Fig. 5. There is only one intense band located in the visible range for both types of the azo polymers, corresponding to the π–π^* electron transition of the pseudo-stilbene azobenzene chromophores [31]. The λ_{max}s of the azo polymers are dramatically affected by the *p*-substituents of the azobenzene moieties. For nitro-substituted PNTAZO, the λ_{max}s are 474 nm in DMF solution and 469 nm as spin-coated film. For cyano-substituted PCNAZO, the λ_{max}s are 447 nm in DMF solution and

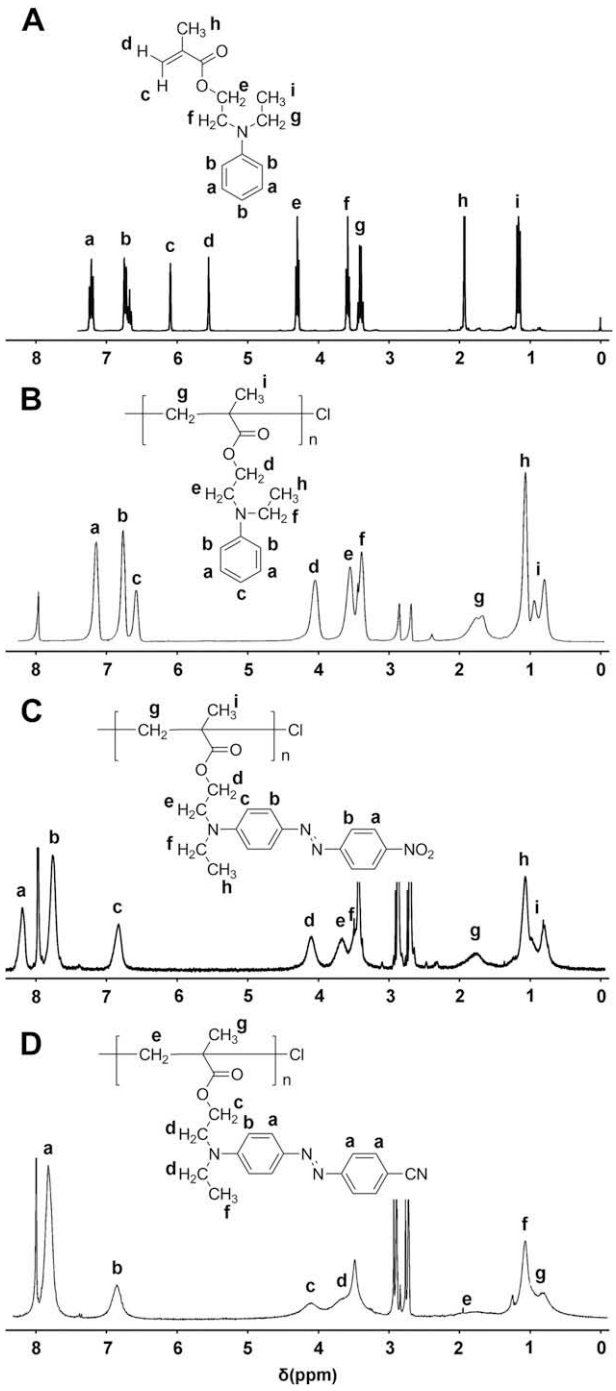

Fig. 3. ^{1}H NMR spectra of (A) monomer EMA in $CDCl_3$ and polymers (B) PEMA (**a1**), (C) PNTAZO (**b1**), (D) PCNAZO (**c1**) in DMF-d_7.

441 nm as spin-coated film. The λ_{max}s of both PNTAZO and PCNAZO as spin-coated films show ca. 5-nm blue shift compared with those of the corresponding DMF solutions. The molar extinction coefficients at 488 nm, estimated from the DMF soltutions, are 2.4×10^6 and 3.0×10^6 M^{-1} cm^{-1} for **b3** and **c3**.

The surface-relief-grating (SRG) formation was studied using the spin-coated thin films of PNTAZO and PCNAZO. The experimental setup and conditions were similar to those reported before [1,2,17], which have been described in Section 2. Although the p-/p- polarization is not as efficient as the oppositely circular polarized beams to write SRGs, this condition can produce good quality

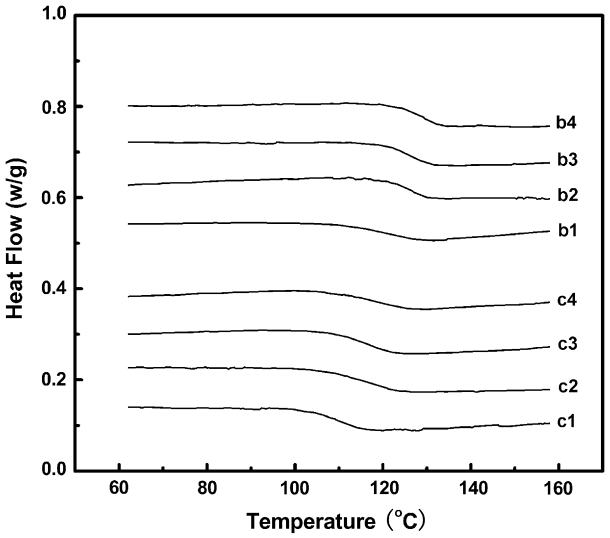

Fig. 4. DSC second-round heating curves of PNTAZO and PCNAZO with different molecular weights.

SRGs and the result is relatively easy to be explained [1–3]. Therefore, the interfering beams with p-/p- polarization were used in this study. Due to the poor solubility, the spin-coated films of **b4** could not form thin film with smooth surface. For the other polymers, thin films with smooth surfaces could be obtained by spin-coating. Upon irradiation of interfering Ar^+ laser beams, sinusoidal surface-relief structures with large surface modulation were formed on the surfaces. Fig. 6 shows the typical AFM surface profiles of the SRGs inscribed on **b2** and **c1** films. The space periods of the gratings (Λ) could be calculated by

$$\Lambda = \lambda/2(\sin\theta)$$

where λ is the wavelength of the writing beam and θ is the angle between the interfering beams [5]. The grating periods measured from AFM profiles can well match the calculated values.

The modulation depth and the inscription rate were recorded to characterize the SRG formation behavior of series of PNTAZO and

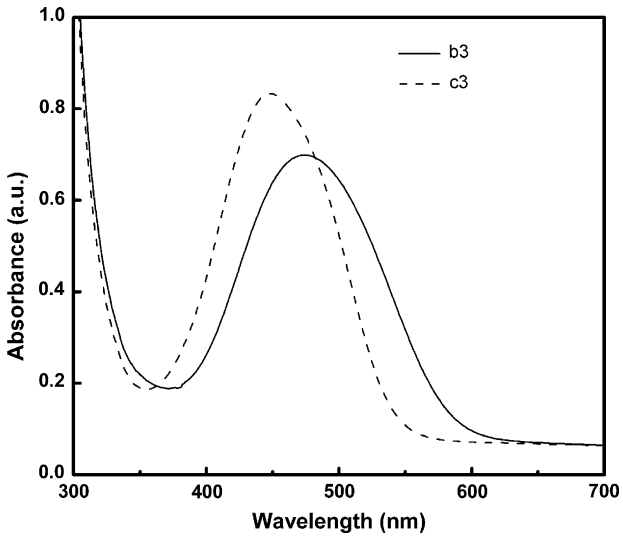

Fig. 5. UV–vis spectra of PNTAZO (**b3**) and PCNAZO (**c3**) in DMF solutions with the concentration of 0.01 mg/mL.

PCNAZO with different M_rs. In the measurements, the polymer film thicknesses were controlled to be almost the same (about 1 μm). The intensity of the Ar^+ laser beam was adjusted to the same value (150 mW/cm^2). The modulation depths of the SRGs were obtained from the AFM profiles. The inscription rates were monitored by measuring the growth of the first-order diffraction efficiency (DE) over time using an unpolarized low-power He–Ne laser beam as the probe beam. After irradiation for 1500 s, the films of **b1**, **b2** and **b3** form SRGs with the modulation depth of about 100 nm. On the other hand, the modulation depths of **c1**, **c2**, **c3** and **c4** films reach about 200 nm after irradiation for 1000 s. The DE growths of the PNTAZO and PCNAZO films are shown in Fig. 7 as a function of the irradiation time. Two important properties can be seen from the figure. First, the azo chromophore structure plays a predominant role in determining the inscription rate. The DE of the PCNAZO film reached 15% after irradiation for 1000 s in contrast to 1.5% of the PNTAZO film after irradiation with the same light intensity for 1500 s. This observation conforms with the modulation depths obtained from AFM measurements. Second, the M_rs of the polymers do not show obvious influence on the inscription rate. The M_r of PCNAZO only shows a minor influence on the inscription rate, which slightly decreases as the M_r increases. For PNTAZO, the M_r influence can almost be ignored due to its triviality.

The effect of electron-withdrawing groups of azo chromophores on the inscription rate has been studied by using polydispersed polymers and low-M_r molecular glass [17,18,20,22]. The current observation based on the narrow-dispersed azo polymers is consistent with those results. In a recent study, the dynamic properties of SRG formation have been studied by considering the correlation between the excitation wavelength (λ_{ex}) and absorption wavelength (λ_{max}) of the azo chromophores [32]. Results show that under conditions of adequate absorbance of the *trans* form at λ_{ex}, the rate of SRG formation increases at longer λ_{ex}. The influence on the SRG formation rate has been attributed to the efficiency of the *trans–cis* photoisomerization cycle [32]. However, at the current stage, the exact isomerization mechanism of azobenzenes is still a debatable issue [33–35]. Because of the overlap of the π–π^* and n–π^* transition bands for the push–pull type azo chromophores, the photoisomerization dynamics depends on the potential energy surfaces through a more complicated way [31,36].

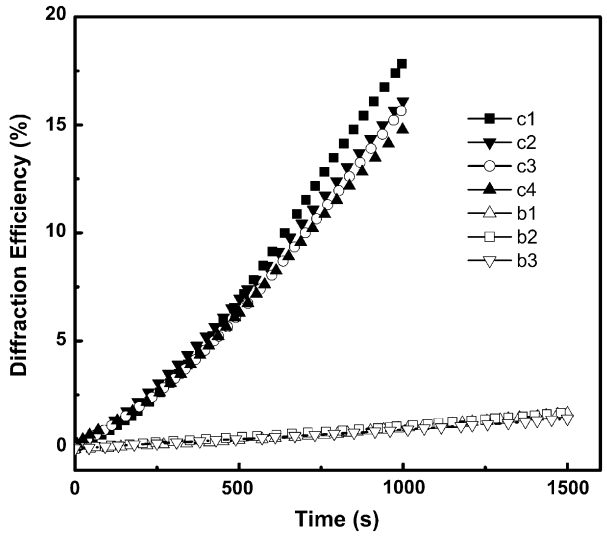

Fig. 7. The first-order diffraction efficiencies of the SRGs inscribed on PNTAZO and PCNAZO films as a function of irradiation time.

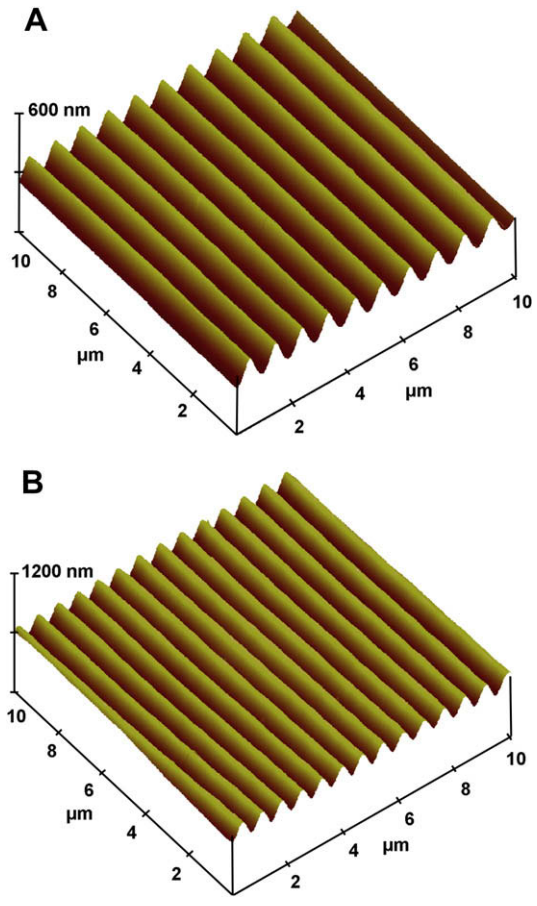

Fig. 6. AFM 3D images of the surface profiles after Ar^+ laser irradiation. (A) PNTAZO (**b2**) film after irradiation for 1500 s, and (B) PCNAZO (**c1**) film after irradiation for 1000 s.

The result that the M_r doesn't show obvious influence on the SRG formation could be rationalized by considering the characteristics of narrow-dispersed azo polymers. In these systems, the azo polymer chains possess almost equal amount of the azo chromophores. Upon light irradiation, the driving force effecting on each molecule should approximately be the same. In this case, the polymer films can be treated more or less as the continuous media, which can be uniformly driven by the light force. The current case is different from the previous studies using blend of PDR1M with PMMA or azo polymers with polydispersity in the composition, sequence structure and M_r [5,19]. For those systems, the inactive components could act as the barriers to the photo-induced chain movement. This effect should increase as the M_r increases.

In the above discussions, the growth of the first-order diffraction efficiency is used to characterize the grating inscription rate, which has also been used in many previous studies [1–6]. A recent report indicates that the diffraction efficiency should at least include the effect from the bulk refractive index grating and the surface-relief-grating [37]. When the diffraction efficiency of both gratings is comparable, the phase shift between the gratings can influence the dynamics of the diffraction efficiency. If the surface modulation is shallow, the correlation between the diffraction efficiency and the real inscription depth can behave in a more complicated manner. On the other hand, the diffraction effect from the bulk refractive index grating can be ignored when the surface modulation is large (such as 200 nm) [38]. Therefore, the correlation between the polymer structure and the SRG inscription rate demonstrated by the diffraction efficiency should be reliable at least for the SRGs with large surface modulation.

4. Conclusion

Two series of narrow-dispersed azo polymers (PNTAZO, PCNAZO), which contain strong push–pull type azobenzene chromophores in side chains, were synthesized by using ATRP and post-polymerization azo-coupling reaction. The azo polymers were characterized by spectroscopic measurements and thermal analysis. The azo polymers prepared were amorphous polymers whose T_gs increased with M_r. SRGs could be inscribed on both PNTAZO and PCNAZO films upon irradiation with the interfering Ar^+ laser beams. Whilst the M_r of PNTAZO and PCNAZO had no effect on the SRG inscription rate, the inscribing rate was significantly influenced by the electron-withdrawing substituents on the azobenzenes.

Acknowledgements

The financial support from NSFC under project 50533040 is gratefully acknowledged.

References

[1] Rochon P, Batalla E, Natansohn A. Optically induced surface gratings on azoaromatic polymer films. Applied Physics Letters 1995;66:136–8.
[2] Kim DY, Tripathy SK, Li L, Kumar J. Laser-induced holographic surface relief gratings on nonlinear optical polymer films. Applied Physics Letters 1995;66:1166–8.
[3] Viswanathan NK, Kim DY, Bian SP, Williams J, Liu W, Li L, et al. Surface relief structures on azo polymer films. Journal of Materials Chemistry 1999;9:1941–55.
[4] Natansohn A, Rochon P. Photoinduced motions in azo-containing polymers. Chemical Reviews 2002;102:4139–75.
[5] Barrett CJ, Natansohn AL, Rochon PL. Mechanism of optically inscribed high-efficiency diffraction gratings in azo polymer films. Journal of Physical Chemistry 1996;100:8836–42.
[6] Kumar J, Li L, Jiang XL, Kim DY, Lee TS, Tripathy SK. Gradient force: the mechanism for surface relief grating formation in azobenzene functionalized polymers. Applied Physics Letters 1998;72:2096–8.
[7] Bian SP, Williams JM, Kim DY, Li LA, Balasubramanian S, Kumar J, et al. Photoinduced surface deformations on azobenzene polymer films. Journal of Applied Physics 1999;86:4498–508.
[8] Lefin P, Fiorini C, Nunzi JM. Anisotropy of the photo-induced translation diffusion of azobenzene dyes in polymer matrices. Pure Applied Optics 1998;7:71–82.
[9] Pedersen TG, Johansen PM, Holme NCR, Ramanujam PS, Hilvsted S. Mean-field theory of photoinduced formation of surface reliefs in side-chain azobenzene polymers. Physical Review Letters 1998;80:89–92.
[10] Tanchak OM, Barrett CJ. Light-induced reversible volume changes in thin films of azo polymers: the photomechanical effect. Macromolecules 2005;38:10566–70.
[11] Yager KG, Tanchak OM, Godbout C, Fritzsche H, Barrett CJ. Photomechanical effects in azo-polymers studied by neutron reflectometry. Macromolecules 2006;39:9311–9.
[12] Yager KG, Barrett CJ. Photomechanical surface patterning in azo-polymer materials. Macromolecules 2006;39:9320–6.
[13] Li XT, Natansohn A, Rochon P. Photoinduced liquid crystal alignment based on a surface relief grating in an assembled cell. Applied Physics Letters 1999;74:3791–3.
[14] Paterson J, Natansohn A, Rochon P, Callender CL, Robitaille L. Optically inscribed surface relief diffraction gratings on azobenzene containing polymers for coupling light into slab waveguides. Applied Physics Letters 1996;69:3318–20.
[15] Cooper SR, Tomkins DW, Petty M. Surface-relief diffraction gratings recorded by multiple-beam coherent phase exposure. Optics Letters 1997;22:357–9.
[16] Fukuda T, Matsuda H, Shiraga T, Kimura T, Kato M, Viswanathan NK, et al. Photofabrication of surface relief grating on films of azobenzene polymer with different dye functionalization. Macromolecules 2000;33:4220–5.
[17] He YN, Wang XG, Zhou QX. Epoxy-based azo polymers: synthesis, characterization and photoinduced surface-relief-gratings. Polymer 2002;43:7325–33.
[18] He YN, Yin JJ, Che PC, Wang XG. Epoxy-based polymers containing methyl-substituted azobenzene chromophores and photoinduced surface relief gratings. European Polymer Journal 2006;42:292–301.
[19] Carvalho LL, Borges TFC, Cardoso MR, Mendonca CR, Balogh DT. Molecular weight effect on the photoinduced birefringence and surface relief gratings formation of a methacrylate azopolymer. European Polymer Journal 2006;42:2589–95.
[20] Ishow E, Lebon B, He YN, Wang XG, Bouteiller L, Galmiche L, et al. Structural and photoisomerization cross studies of polar photochromic monomeric glasses forming surface relief gratings. Chemistry of Materials 2006;18:1261–7.
[21] Nakano H, Tanino T, Takahashi T, Ando H, Shirota Y. Relationship between molecular structure and photoinduced surface relief grating formation using azobenzene-based photochromic amorphous molecular materials. Journal of Materials Chemistry 2008;18:242–6.
[22] He YN, Gu XY, Guo MC, Wang XG. Dendritic azo compounds as a new type amorphous molecular material with quick photoinduced surface-relief-grating formation ability. Optical Materials 2008;31:18–27.
[23] Matyjaszewski K, Xia JH. Atom transfer radical polymerization. Chemical Reviews 2001;101:2921–90.
[24] Wang DR, Ye G, Wang XG. Synthesis of aminoazobenzene-containing diblock copolymer and photoinduced deformation behavior of its micelle-like aggregates. Macromolecular Rapid Communications 2007;28:2237–43.
[25] Natansohn A, Rochon P, Gosselin J, Xie S. Azo polymers for reversible optical storage. 1. Poly[4′-[[2-(acryloyloxy)ethyl]ethylamino]-4-nitroazobenzene]. Macromolecules 1992;25:2268–73.
[26] Ding LM, Russell TP. A photoactive polymer with azobenzene chromophore in the side chains. Macromolecules 2007;40:2267–70.
[27] Wang XG, Chen JI, Marturunkakul S, Li L, Kumar J, Tripathy SK. Epoxy-based nonlinear optical polymers functionalized with tricyanovinyl chromophores. Chemistry of Materials 1997;9:45–50.
[28] Wang XG, Kumar J, Tripathy SK, Li L, Chen JI, Marturunkakul S. Epoxy-based nonlinear optical polymers from post azo coupling reaction. Macromolecules 1997;30:219–25.
[29] Gan LH, Ravi P, Mao BW, Tam KC. Controlled/living polymerization of 2-(diethylamino)ethyl methacrylate and its block copolymer with *tert*-butyl methacrylate by atom transfer radical polymerization. Journal of Polymer Science Part A: Polymer Chemistry 2003;41:2688–95.
[30] Matsuyama M, Kamigaito M, Sawamoto M. Sulfonyl chlorides as initiators for the ruthenium-mediated living radical polymerization of methyl methacrylate. Journal of Polymer Science Part A: Polymer Chemistry 1996;34:3585–9.
[31] Rau H. In: Rabek JF, editor. Photochemistry and Photophysics, vol. II. Boca Raton: CRC Press; 1990 [chapter 4].
[32] Kim MJ, Lee JD, Chun C, Kim DY, Higuchi S, Nakayama T. Control of photodynamic motions of azobenzene-derivative polymers by laser excitation wavelength. Macromolecular Chemistry and Physics 2007;208:1753–63.
[33] Fliegl H, Kohn A, Hattig C, Ahlrichs R. Ab initio calculation of the vibrational and electronic spectra of *trans*- and *cis*-azobenzene. Journal of the American Chemical Society 2003;125:9821–7.
[34] Chang CW, Lu YC, Wang TT, Diau EWG. Photoisomerization dynamics of azobenzene in solution with S-1 excitation: a femtosecond fluorescene anisotropy study. Journal of the American Chemical Society 2004;126:10109–18.
[35] Lu YC, Diau EWG, Rau H. Femtosecond fluorescence dynamics of rotation-restricted azobenzenophanes: a new evidence on the mechanism of *trans–cis* photoisomerization of azobenzene. Journal of Physical Chemistry 2005;109:2090–9.
[36] Schmidt B, Sobotta C, Malkmus S, Laimgruber S, Braun M, Zinth W, et al. Femtosecond fluorescence and absorption dynamics of an azobenzene with a strong push–pull substitution. Journal of Physical Chemistry 2004;108:4399–404.
[37] Sobolewska A, Miniewicz A. Analysis of the kinetics of diffraction efficiency during the holographic grating recording in azobenzene functionalized polymers. Journal of Physical Chemistry B 2007;111:1536–44.
[38] Labarthet FL, Buffeteau T, Sourisseau C. Analyses of the diffraction efficiencies, birefringence, and surface relief gratings on azobenzene-containing polymer films. Journal of Physical Chemistry B 1998;102:2654–62.